Molecular Pharmacology 107 (2025) 100008

Molecular Pharmacology

journal homepage: www.molpharm.aspetjournals.org

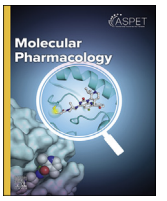

ARTICLE

High-throughput screening identifies a novel small-molecule modulator of Hsp70 that selectively enhances ubiquitination and degradation of misfolded neuronal NO synthase

Anthony M. Garcia [1], Amanda K. Davis [1], Cristian Martinez-Ramos [1], Yoshihiro Morishima [1], Miranda Lau [1], Emily Xu [1], Arya Sunil [1], Haoming Zhang [1], Andrew Alt [1,2], Andrew P. Lieberman [3], Yoichi Osawa [1,*]

[1] Department of Pharmacology, University of Michigan Medical School, Ann Arbor, Michigan
[2] Center for Chemical Genomics, Life Sciences Institute, University of Michigan, Ann Arbor, Michigan
[3] Department of Pathology, University of Michigan Medical School, Ann Arbor, Michigan

ARTICLE INFO

Article history:
Received 23 July 2024
Accepted 19 November 2024
Available online 12 December 2024

Key words:
Chaperone
Hsp70
Ubiquitination
Protein quality control
Degradation

ABSTRACT

The Hsp90 and Hsp70 chaperones act as a protein quality control system for several hundred client proteins, including many implicated in neurodegenerative disorders. Hsp90 and Hsp70 are widely thought to be important drug targets. Although many structurally distinct compounds have been developed to target Hsp90, relatively few are known to target Hsp70 and even fewer have been tested in protein quality control systems. To address this, we describe a high-throughput thermal shift-based screen to find compounds that bind and stabilize Hsp70 and then employ assays with misfolded forms of a well-established client protein, neuronal NO synthase (nNOS), to identify compounds that enhance ubiquitination of client proteins. The ubiquitination assay employed a quantitative ELISA method to measure Hsp70:CHIP-dependent ubiquitination of heme-deficient nNOS, which is a model of a misfolded client, in reaction mixtures containing purified E1, E2, Hsp70, CHIP, and ubiquitin. We screened 44,447 molecules from the Maybridge and ChemDiv libraries and found one compound, protein folding disease compound 15 (PFD-15), that enhanced in vitro nNOS ubiquitination with an EC_{50} of approximately 8 μM. PFD-15 was tested in human embryonic kidney 293 cells stably transfected with a C331A nNOS, a mutation that makes nNOS a preferred client protein for ubiquitination. In this model, PFD-15 decreased steady-state levels of C331A nNOS, but not the wild-type nNOS, in a time- and concentration-dependent manner by a process attenuated by lactacystin, an inhibitor to the proteasome. PFD-15 appears to enhance binding of Hsp70 and CHIP to client proteins without interference of protein quality control mechanisms, enabling the selective clearance of misfolded proteins.

Significance Statement: There are few treatment options for neurodegenerative diseases, which are widely thought to be caused by formation of toxic misfolded proteins. One novel approach is to enhance the Hsp90/Hsp70 protein quality control machinery to remove these misfolded proteins. Targeting Hsp70 may have advantages over targeting Hsp90, but fewer compounds targeting Hsp70 have been developed relative to those for Hsp90. The current study provides a novel approach to enhance the number of compounds targeting the Hsp70's role in protein quality control.

1. Introduction

The heat shock protein 90 (Hsp90) and heat shock protein 70 (Hsp70) chaperone system regulates protein quality control for over a hundred client proteins, including those implicated in neurodegenerative disease (Pratt et al, 2015; Gong et al, 2016; Davis

* **Address correspondence to:** Dr Yoichi Osawa, Department of Pharmacology, University of Michigan Medical School, Medical Sciences Building III, Ann Arbor, MI 48109. E-mail: osawa@umich.edu

This article has supplemental material available at molpharm.aspetjournals.org.

A.M.G. and A.K.D. contributed equally to this work as first authors.

https://doi.org/10.1016/j.molpha.2024.100008
0026-895X/

et al, 2020b; Gupta et al, 2020). Hsp90 and Hsp70 play opposing roles in the regulation of client protein degradation; Hsp90 stabilizes and protects proteins from degradation, whereas Hsp70 facilitates the ubiquitination of client proteins by chaperone-associated E3 ligases such as C-terminus of Hsp70 interacting protein (CHIP). We have previously demonstrated with neuronal NO synthase (nNOS), a well-characterized client protein, that overexpression of an Hsp70 cochaperone Hsp70 interacting protein (HIP) stabilizes an ADP-bound conformation of Hsp70 and enhances nNOS ubiquitination (Wang et al, 2013). Overexpression of HIP also increased clearance of other client proteins, including a polyglutamine tract containing androgen receptor (polyQ-AR), the causative agent in a protein misfolding and aggregation neurodegenerative disease known as spinobulbar muscular atrophy. Moreover, YM-01, an allosteric modulator of Hsp70 that works in a manner similar to HIP, also increases polyQ-AR and nNOS ubiquitination. Most importantly, either overexpression of HIP or YM-01 treatment alleviated toxicity in a polyQ-AR *Drosophila* model of spinobulbar muscular atrophy (Wang et al, 2013). The targeting of Hsp70-facilitated protein quality control for treatment of polyglutamine diseases has been proposed (Pratt et al, 2015; Davis et al, 2020b; Venediktov et al, 2023). Thus, there is interest in the development of modulators that activate Hsp70-dependent ubiquitination and degradation for therapeutic use.

Although many compounds that directly inhibit Hsp90 have been developed and tested in over 70 clinical trials (Talaei et al, 2019; Mehta et al, 2020; Li and Luo, 2023), fewer compounds have been developed to directly target Hsp70 (Lazarev et al, 2018; Shao et al, 2018; Gestwicki and Shao, 2019; Ambrose and Chapman, 2021). Moreover, nearly all of these efforts have been directed at developing anticancer agents, with very few directed at neurodegenerative diseases (Davis et al, 2020b). In those studies, phenothiazine compounds, such as methylene blue, that inhibit the ATPase activity of Hsp70 (Wang et al, 2010), as well as rhodacyanine dyes, such as MKT-077, YM-01, and JG-98, that are allosteric modulators of Hsp70 have been investigated for neurodegenerative diseases (Wang et al, 2013; Young et al, 2016; Davis et al, 2020b; Shao et al, 2021). These 2 classes of compounds have been found to have other off-target effects (Congdon et al, 2012; Echtenkamp et al, 2023); thus, there is interest in screening approaches that could be used to find new classes of compounds directed at Hsp70-dependent protein quality control functions.

In the current study, we used a high-throughput Hsp70 thermal shift assay along with misfolded nNOS in in vitro and cellular assays to screen 44,447 molecules from a structurally diverse library. The use of this set of novel assays identified a compound, protein folding disease compound 15 (PFD-15), that selectively enhances Hsp70-dependent ubiquitination and degradation of misfolded forms of nNOS while sparing the native enzyme. PFD-15 is a novel molecule that has not been previously described to interact with Hsp70 or to enhance degradation of nNOS. Expansion of this screening method to a larger number of compounds is likely to identify other structurally diverse candidates for further study with other important client proteins.

2. Materials and methods

2.1. Materials

1-Step slow 3,3',5,5'-tetramethylbenzidine—ELISA substrate solution (catalog number 34024), radioimmunoprecipitation assay (RIPA) lysis and extraction buffer (catalog number 89901), and SYPRO Orange protein gel stain (5000X concentrate in DMSO, catalog number S6651) were purchased from Thermo Fisher Scientific. ATP disodium salt hydrate (catalog number A1852) and ADP sodium salt (catalog number A2754) were purchased from Sigma-Aldrich. Radicicol was purchased from Cayman Chemical (catalog number 13089). A horseradish peroxidase (HRP)—conjugated antibody that recognizes monoubiquitinylated and polyubiquitinylated conjugates (FK2, catalog number BML-PW0150-0025, RRID:AB_2051892) was purchased from Enzo Life Sciences. DYKDDDDK-tag (FLAG) Antibody Plate (Clear, 8X12 strip catalog number L00455C) was purchased from GenScript. Rabbit reticulocyte lysate was purchased from Green Hectares. Ubiquitin-activating enzyme E1 was purchased from R&D Systems (catalog number E-305-025). The cDNA for expressing the glutathione *S*-transferase—tagged UbcH5a (E2, ubiquitin carrier protein) was kindly provided by C.M. Pickart (Johns Hopkins Medical School, Baltimore, Maryland). cDNA for His-CHIP was kindly provided by C. Patterson (University of North Carolina, Chapel Hill). The cDNA for rat nNOS was kindly provided by Dr Solomon Snyder (The Johns Hopkins Medical School, Baltimore). The cDNA for His-HA—tagged ubiquitin was from Dr Yi Sun (University of Michigan, Ann Arbor). Human Hsp70 cDNA was kindly provided by Dr David Toft (Mayo Clinic, Rochester, Minnesota). JG-98 (2-[(*Z*)-[(5E)-5-(6-chloro-3-methyl-2(3H)-benzothiazolylidene)-3-ethyl-4-oxo-2-thiazolidinylidene]methyl]-3-(phenylmethyl)-thiazolium, monochloride) was kindly provided by Jason Gestwicki (University of California, San Francisco, California). YM-01 (2-[[3-Ethyl-5-(3-methyl-2(3H)-benzothiazolylidene)-4-oxo-2-thiazolidinylidene]methyl]-1-methyl-pyridinium chloride) was purchased from Sigma-Aldrich (catalog number SML0943). Compounds selected from the high-throughput screen for additional studies were purchased from Molport. Dulbecco's modified Eagle's medium (DMEM, catalog number 11995-065) and Geneticin (catalog number 10-1310035) were purchased from Gibco. FBS (catalog number SH30071.03) was purchased from HyClone. Hygromycin B (catalog number 10687010) was purchased from Invitrogen.

2.2. Expression and purification of proteins

Glutathione *S*-transferase—tagged UbcH5a was bacterially expressed and purified by glutathione-Sepharose (Sigma-Aldrich) affinity chromatography, as previously described (You and Pickart, 2001). His-CHIP and His-HA-ubiquitin were bacterially expressed and purified by nickel-nitrilotriacetic acid affinity chromatography, as previously described (Ballinger et al, 1999). Hsp70 was bacterially expressed and purified by ATP-agarose chromatography, adapted from Dittmar et al (1996). Hsp90 was purified from rabbit reticulocyte lysate by sequential chromatography on DE52, hydroxyapatite, and ATP-agarose, as previously described (Dittmar et al, 1996). FLAG—apo-nNOS (Morishima et al, 2016) was made by expression in Sf9 insect cells using a recombinant baculovirus and purification by 2′,5′-ADP-Sepharose and gel-filtration chromatography, as described previously (Bender et al, 1999).

2.3. Fluorescence thermal shift assay

Medium-throughput 96-well format was as follows: the melting temperature (Tm) of Hsp70 was determined by a fluorescence thermal shift assay using SYPRO Orange dye (λ_{ex} 470 nm/λ_{em} 570 nm). A mixture of Hsp70 (1.5 μM), SYPRO Orange (10×), and the small molecule to be tested was prepared in a buffer containing 50 mM potassium phosphate pH 7.4, 300 mM KCl, and 10% glycerol in a total volume of 25 μL. A CFX96 Real-Time PCR System (Bio-Rad) was used to heat samples from 25 °C to 99 °C with a temperature increase of 0.3 °C per minute while simultaneously measuring fluorescence. The Tm of the resulting melting curve was determined using CFX Manager (Bio-Rad). The Hsp90 thermal shift assay was carried out under the same conditions, except that purified Hsp90 (1.5 μM) was used in place of Hsp70.

High-throughput 384-well format was as follows: the thermal shift assay was adapted to a high-throughput 384-well plate format, and 44,447 compounds from the Maybridge and ChemDiv collection at the Center for Chemical Genomics were screened at 50 μM under the same conditions described above, except that the final volume was 10 μL. A QuantStudio 7 Flex Real-Time PCR System (Thermo Fisher Scientific) was used to heat samples from 25 °C to 80 °C with a temperature increase of 0.03 °C per second while simultaneously measuring fluorescence. Protein Thermal Shift Software 1.3 (Thermo Fisher Scientific) was used to determine the Tm of the resulting melting curves. Samples treated with DMSO or 1 mM ADP were used as negative and positive controls, respectively. A Z-factor was calculated as previously described (Zhang et al, 1999). The compounds were evaluated as a percentage of their respective Tm relative to the positive control Tm. An increase in Tm greater than 3.5 SDs of the negative control was considered a positive hit.

2.4. In vitro ubiquitination of nNOS

A ubiquitination reaction mixture containing purified FLAG–apo-nNOS (0.2 μM), Hsp70 (1 μM), His-CHIP (1 μM), E2 ubiquitin–conjugating enzyme (1 μM), ubiquitin-activating enzyme E1 (0.1 μM), His-HA-ubiquitin (100 μM), and ATP (100 μM) in a total volume of 20 μL of 50 mM Hepes pH 7.4, 100 mM KCl, and 5 mM dithiothreitol was incubated for 15 minutes, unless specified otherwise, at 22 °C. Reactions were then diluted in RIPA buffer to a final FLAG–apo-nNOS concentration of 0.03 μM, and 100 μL was added per well to an anti-FLAG 96-well plate. The plate was incubated for 4 hours at 4 °C and then washed 3 times with RIPA buffer and once with PBS. Wells were treated with a 100 μL solution of antiubiquitin antibody conjugated to HRP (1:2000) in PBS. The plate was incubated for 1 hour at room temperature and then washed 3 times with PBS containing 1% Tween 20 (Sigma-Aldrich) and once with PBS. Wells were treated with 100 μL of 3,3',5,5'-tetramethylbenzidine, and absorbance at 370 nM was measured every 15 seconds for 120 seconds. HRP activity was calculated by linear regression. HRP activity was corrected for the nNOS-independent signal, normalized to untreated control, and reported as nNOS ubiquitination.

2.5. Cell culture and western blotting

Flp-In 293 cells (catalog number R75007, Invitrogen, RRID:CVCL_U421) were transfected with C331A nNOS cDNA using Lipofectamine 3000 (catalog number 18324012, Invitrogen). Stable cell lines were selected for hygromycin B resistance by picking single colonies and expanding in the selection medium (DMEM, 10% FBS, and 0.5 mg/mL hygromycin B). These cells were then maintained in DMEM with 10% FBS and 0.1 mg/mL hygromycin B. Cells stably expressing wild-type nNOS (previously described in Bredt et al, 1991) were cultured in DMEM supplemented with 10% FBS and Geneticin (0.5 mg/mL). Cell cultures were routinely inspected for possible mycoplasma contamination.

Before experimentation, cells were replated in 12-well plates, cultured in DMEM with 10% FBS, and allowed to incubate for 2 days. Cells were treated when wells reached 80%–90% confluency and incubated for the indicated time. Where indicated, lactacystin (catalog number BML-PI104-1000, Enzo Life Sciences) or bafilomycin A1 (catalog number SML1661, Sigma-Aldrich) was used to pretreat cells before PFD-15 treatment. Cells were then harvested following treatment via mechanical detachment, washed with ice-cold PBS, centrifuged (500 $\times$ g for 5 minutes at room temperature), and the cell pellet was resuspended in 0.1 mL RIPA buffer supplemented with 2.5 mM phenylmethylsulfonyl fluoride and Roche cOmplete Mini Protease Inhibitor Cocktail (catalog number 11836170001, Sigma-Aldrich) before sonication. Homogenates were centrifuged at 4 °C for 15 minutes at 15,000 $\times$ g, with the supernatant being collected as the cytosol fraction. Total protein concentration was determined using the Pierce BCA Protein Assay Kit (catalog number 23225, Thermo Fisher Scientific). Equal amounts of total protein (5 μg) in 2$\times$ Laemmli buffer were electrophoresed through 4%–20% gradient SDS-polyacrylamide gels (catalog number 4561096, Bio-Rad) and transferred to polyvinylidene fluoride membranes using a wet-transfer apparatus. Before probing for target protein levels, membranes were stained with Revert 700 Total Protein Stain (LI-COR Biosciences, catalog number 926-11016), and the total protein signal for each lane was detected in a LI-COR Odyssey FC imager. Following total protein stain removal, Hsp70 and nNOS protein levels were probed with mouse anti-Hsp70 (Enzo Life Sciences, catalog number SPA-810-488D, RRID:AB_1083494, N23F3-4, 1:2000) and rabbit anti-nNOS (Sigma-Aldrich, catalog number SAB4502010, RRID:AB_10744459, N2780, 1:5000) incubated overnight, followed by 1-hour incubation with the fluorescent secondary antibodies anti-Ms 800 (LI-COR Biosciences, catalog number 925-32210, RRID:AB_2687825, 1:2000) and goat anti-Rb 680 (LI-COR Biosciences, catalog number 926-68071, RRID:AB_10956166, 1:50,000). The relative intensity of the bands was quantified in Image Studio from LI-COR Biosciences and corrected using the total protein stain signal as described by the manufacturer.

Flp-In 293 T-Rex cells (catalog number R78007, Invitrogen, RRID:CVCL_U427) were used to cotransfect wild-type nNOS-FLAG constructs to make a tetracycline-inducible cell line to express FLAG-tagged nNOS according to the manufacturer's directions. To make heme-deficient apo-nNOS, the cells were pretreated with succinylacetone (500 μM) for 2 hours in DMEM containing 10% heme-depleted FBS as described (Zhu et al, 2002) and then treated with tetracycline (1 μg/mL) for 24 hours. No detectable nNOS activity was present as assessed by the oxyhemoglobin assay (data not shown), but nNOS was detected by western blotting. Cells were then treated with PFD-15 (40 μM) for 2 hours. The FLAG-tagged nNOS was immunoprecipitated and western blotted with 2 μg/mL mouse anti-Hsp70 (N23F3-4, 1:2000) as described (Morishima et al, 2023). CHIP was immunoblotted with rabbit anti-CHIP antiserum (Millipore, catalog number PC711, RRID:AB_2198058, 1:2500 v/v).

Human embryonic kidney 293 (HEK293)T cells (catalog number CRL-3216, ATCC, RRID:CVCL_0063) not transfected with nNOS were grown in DMEM supplemented with 10% FBS in 6-well plates. Cells were pretreated with DMSO or PFD-15 (40 μM) for 30 minutes at 37 °C. The media was aspirated and replaced with media (1.5 mL) prewarmed to 37 °C or 42 °C containing vehicle or PFD-15 (40 μM) and further incubated at 37 °C or 42 °C for 30 minutes. Cells were harvested and western blotted as described above, except they were probed with a mouse antiubiquitin antibody that recognizes monoubiquitinylated and polyubiquitinylated conjugates (Enzo Life Sciences, catalog number SPA-205E, RRID:AB_311908, FK2, 1:1000).

2.6. Heterocomplex assembly of Hsp70 and CHIP onto immobilized apo-nNOS in vitro

To form heterocomplexes in vitro, Hsp70 (0.6 μM), CHIP (0.6 μM), and PFD-15 (0, 40, or 80 μM) were preincubated in HKD buffer (10 mM Hepes, pH 7.35, 100 mM KCl, and 0.1 mM dithiothreitol) in the presence of ARS (10 mM Hepes, pH7.4, 50 mM ATP, 250 mM creatine phosphate, 20 mM magnesium acetate, and 100 units/mL creatine phosphokinase) for 20 minutes at 4 °C. This mixture was then incubated with immobilized apo-nNOS (0.6 μM) for 20 minutes at 30 °C, similar to that described previously (Morishima et al, 2023). The apo-nNOS was eluted with FLAG peptide and eluant

blotted for Hsp70 and CHIP as described above. In some experiments, Bag-1M (5 μM) was added to the preincubation reaction mixture as previously described (Davis et al, 2020a).

2.7. Statistical analysis

We conducted exploratory studies of the effects of novel compounds on Hsp70 and Hsp90 thermostability, as well as Hsp70:CHIP-dependent ubiquitination of nNOS. As such, calculated *P* values for these experiments can only be interpreted as descriptive. Statistical analysis was performed with GraphPad Prism version 10.2.2 (GraphPad); comparisons were made by one-way ANOVA, and curves were fitted with either a nonlinear sigmoidal 4-parameter logistic regression or the Boltzmann Sigmoid linear regression. Multiple comparisons posttests were performed where indicated in figure legends, and groups selected for comparison were chosen before the data had been viewed. For all western blots from cell experiments (not including immunoprecipitation experiments), values of probed proteins were corrected based on total protein stain signal.

3. Results

3.1. Thermal shift assay to identify small molecules that bind and thermostabilize Hsp70

We used a thermal shift assay to screen 44,447 compounds from a library containing chemicals from the Maybridge and ChemDiv libraries as the first step in identifying compounds that bind and thermostabilize Hsp70 (Fig. 1). As shown in Fig.2A, we used a SYPRO Orange–based fluorescence assay to monitor the thermostability of purified Hsp70 (solid line). The addition of 1 mM ADP (dashed line) gives a rightward shift to the curve, indicating a stabilization of Hsp70 against heat denaturation, consistent with previous reports using circular dichroism and inherent protein fluorescence measurements (Palleros et al, 1994). A convenient measure of Hsp70 thermostability is the Tm, which is defined as the inflection point of the melting curve as indicated (dotted line). The primary screening data have been included in Supplemental Table 1. As shown in Fig. 2B, ADP caused a concentration-dependent increase in the Tm of Hsp70 from 46 °C to 54 °C. Capitalizing on this robust window, we next developed a high-throughput assay on a 384-well format to screen the 2 libraries. We determined a Z-factor of 0.8 with the use of 1 mM ADP as a positive control (Fig. 2C). Compounds were tested at 50 μM in quadruplicate, and those that caused an increase in Tm (as percentage response of the positive control) greater than 3.5 SDs from the untreated sample were considered positive in this assay; 2126 positives were identified resulting in a hit ratio of 4.8%. As shown in Fig. 1, the compounds that showed a positive response at least 3 out of 4 times were selected, resulting in 704 compounds. These hits were retested, and 129 were found to produce a concentration-dependent response. Cluster analysis of the 129 compounds gave 76 clusters. We prioritized compounds with the highest efficacy and potency from each cluster and used pan-assay interference compound filters and commercial availability to select 35 compounds for repurchase. For validation, the repurchased compounds were tested for a concentration-response from 100 nM to 500 μM. Of the 35 repurchased compounds, 16 caused an increase in Tm of Hsp70 greater than 3 SDs of the untreated control, leading to a minimum Tm change of 0.8 °C (Table 1).

3.2. Hsp90 counter screen to evaluate Hsp70 thermostabilizer selectivity

An Hsp90 counter screen was used to investigate the selectivity of the Hsp70 thermostabilizers identified by the high-throughput screening. This assay is identical to the Hsp70 thermal shift assay above, except that purified Hsp90 replaced Hsp70. As shown in Fig. 3A, the addition of 10 μM of the known Hsp90 inhibitor, radicicol, caused a rightward shift in the melting curve of Hsp90 (dashed line vs solid line). We observed that the melting curve of Hsp90 incubated with radicicol had 2 phases, with a shoulder just left of the peak. The Tm was determined by the inflection point of the second phase. More importantly, we observed that radicicol had no effect on the Tm Hsp70 (Fig. 3B). The 16 validated Hsp70 thermostabilizers were tested for a concentration-dependent response in this Hsp90 counter screen, and any compound

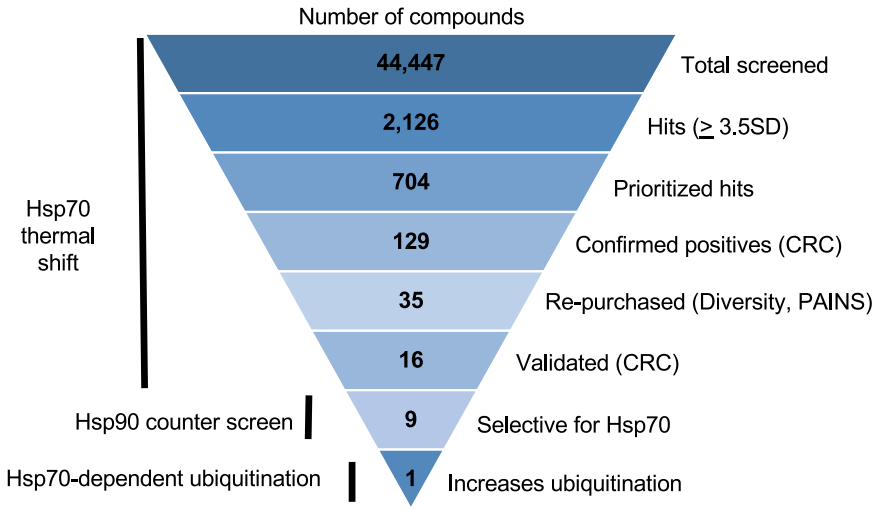

Fig. 1. Overview of the screening for molecules that modulate Hsp70 and increase the Hsp70:CHIP-dependent ubiquitination of nNOS. A thermal shift assay was used to screen a chemical library (44,447 compounds) for thermostabilizers of Hsp70. Hits (2126 compounds) were selected (>3.5 SDs of DMSO control) and prioritized for reproducibility, selecting compounds that hit at least 3 out of 4 replicates to give 704 compounds. These hits were confirmed by concentration-response curves (CRCs), leaving 129 compounds. Based on structural similarity and pan-assay interference compounds (PAINS) filtering, 35 compounds representing unique structural classes were selected for repurchase and validated by CRC (16 compounds). An Hsp90 thermal shift counter screen was then used to eliminate nonselective hits, leaving 9 compounds. Only 1 of these 9 compounds exhibited increased Hsp70:CHIP-dependent nNOS ubiquitination with the use of an in vitro assay.

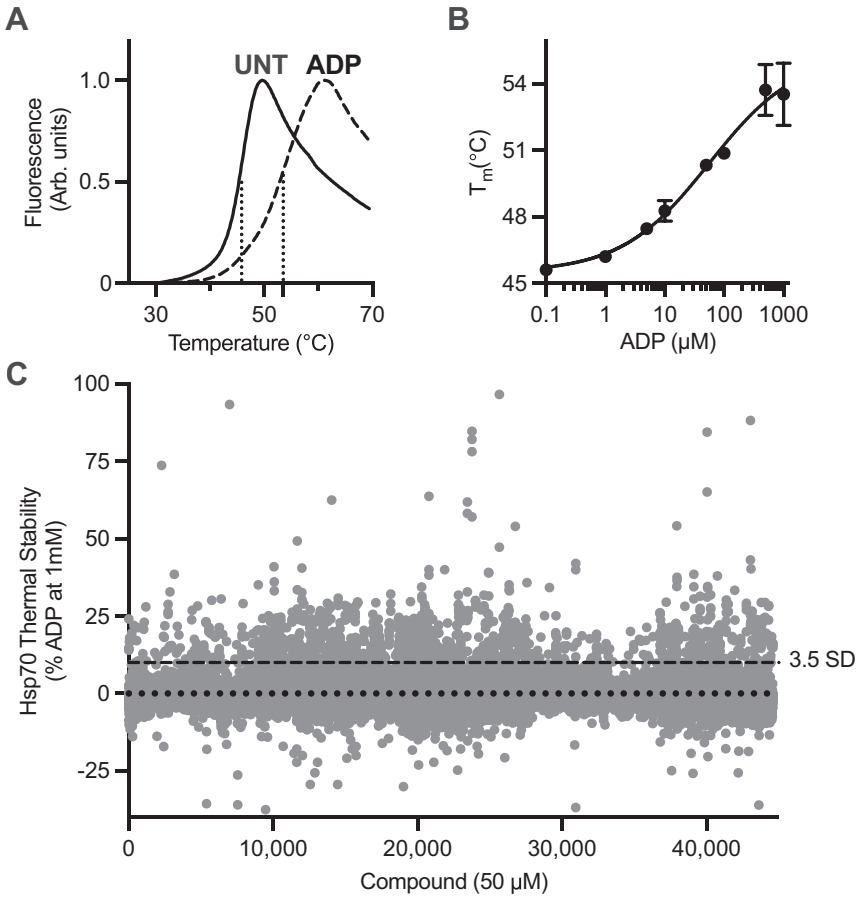

Fig. 2. Thermal shift assay to screen for compounds that bind to Hsp70, using purified Hsp70 and the fluorescent dye SYPRO Orange. (A) ADP enhances the thermal stability of Hsp70. Representative melting curves for Hsp70 untreated (UNT, solid line) or treated with 1 mM ADP (ADP, dashed line). (B) Concentration-dependence of ADP on the Tm of Hsp70. The Tm values were calculated by determining the inflection point on each melting curve and reported as mean ± SD ($n = 3$). (C) A total of 44,447 compounds were screened by the Hsp70 thermal shift assay adapted to a high-throughput platform. Results are plotted as a percentage of the value for 1 mM ADP. Compounds that caused a change in Tm greater than 3.5 SDs of the control were considered positive (dashed line). The Z-factor for the high-throughput assay is 0.80. Arb. units, arbitrary units.

exhibiting a change in Tm greater than 3 SDs from untreated Hsp90 was excluded (Table 1). We were left with 9 positives that demonstrated selectivity for Hsp70 (Table 1, highlighted in gray). The Hsp70 thermal shift data for these 9 hits are shown in Fig. 4, with representative melt curves shown in Supplemental Fig. 1. Five of these compounds (Fig. 4, C, D, F, G, and I) exhibited an increase in Hsp70 Tm by ~1 °C at the highest concentration of the compound tested. Three of the compounds (Fig. 4, A, B, and H) increased Hsp70 thermostability by ~2 °C, with PFD-15 (Fig. 4E) having the highest increase in Tm of over 3 °C.

Table 1
Small-molecule Hsp70 thermostabilizers identified by high-throughput screening
Thermostabilizers selective for Hsp70 are highlighted in gray. Calculated pEC_{50} values were determined by the results of 3 independent experiments ($n = 3$).

Compound	Hsp70 Thermal Shift Assay		Hsp90 Counter Screen	
	ΔTm	pEC_{50}	ΔTm	pEC_{50}
	°C		°C	
PFD-1	1.0	4.2	2.6	4.6
PFD-2	1.8	4.8		
PFD-4	2.4	3.5		
PFD-5	1.9	4.9	15.2	4.5
PFD-6	1.0	4.6		
PFD-10	0.9	4.9	2.3	5.4
PFD-12	0.9	4.3		
PFD-15	3.4	4.1		
PFD-16	1.1	4.3		
PFD-24	1.0	4.6	8.8	4.9
PFD-26	0.7	3.9	5.6	4.8
PFD-30	2.5	4.8	7.7	5.4
PFD-31	0.8	5.0		
PFD-32	1.3	<3.3	7.7	4.5
PFD-33	1.9	4.1		
PFD-35	0.9	5.0		

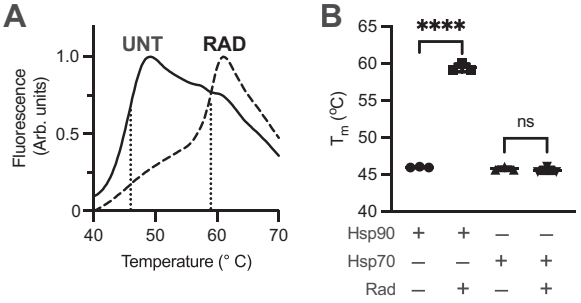

Fig. 3. Hsp90 thermal shift counter screen to investigate selectivity of Hsp70 thermostabilizers. (A) Thermal shift counter screen using purified Hsp90 and the fluorescent dye SYPRO Orange. Hsp90 was untreated (UNT, solid line) or treated with an Hsp90 inhibitor, 10 μM radicicol (RAD, dashed line). (B) Effect of RAD (10 μM) on the Tm of Hsp90 and Hsp70. Values are reported as Tm averages ± SD ($n = 3$). Ordinary one-way ANOVA followed by Šídák's multiple comparisons test was used to evaluate the effect of RAD treatment on each protein's thermal stability. ****$P < .0001$. Arb. units, arbitrary units; ns, not significant.

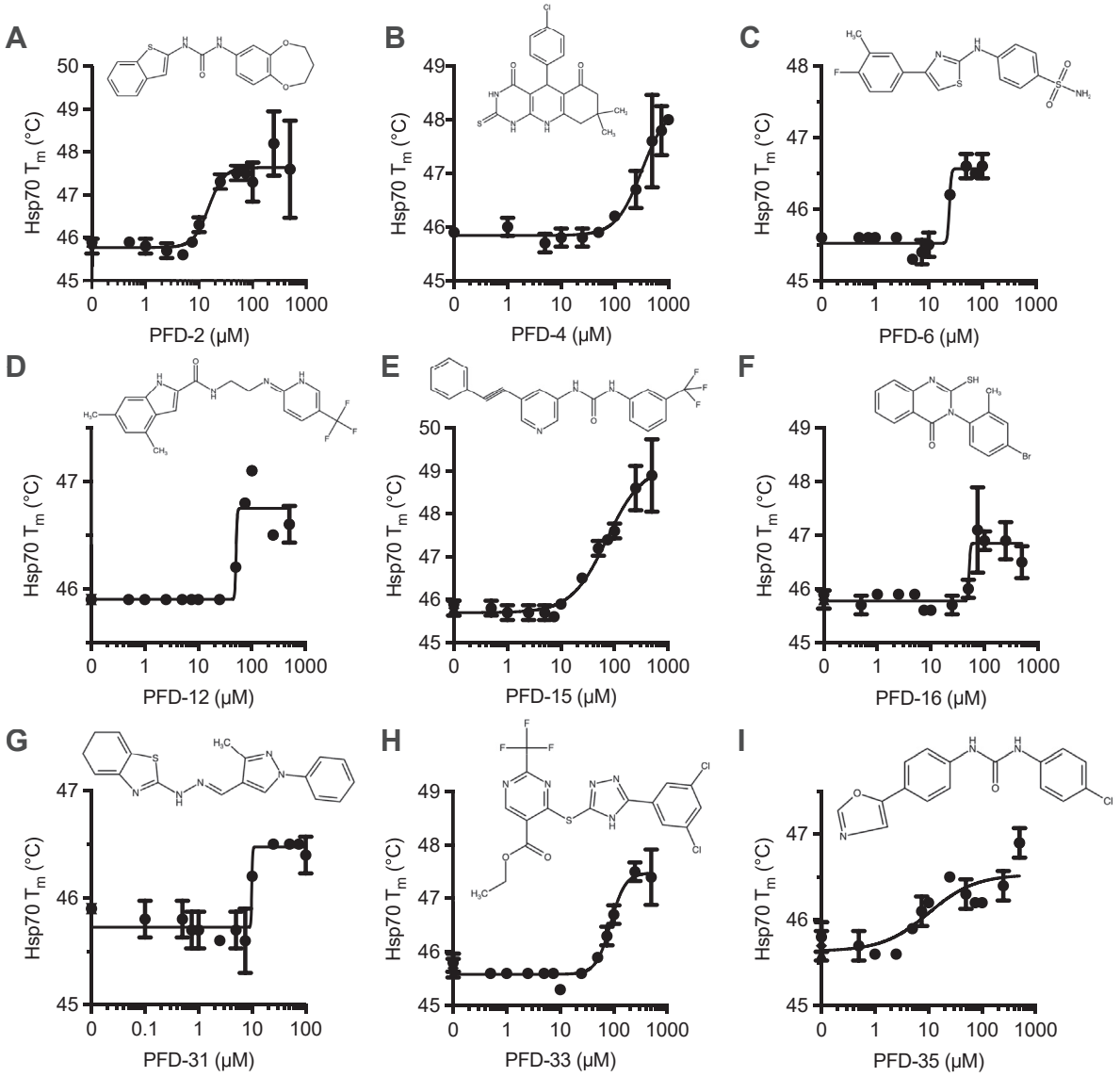

Fig. 4. Nine compounds increase Hsp70 Tm. Nine compounds were found to increase Hsp70 thermostability (A–I) in a concentration-dependent manner without affecting Hsp90 Tm (Table 1). Values are reported as Tm means ± SD ($n = 3$).

Following the Hsp90 counter screen, we compared the Hsp70 melt curves of the Hsp70 selective compounds (Supplemental Fig. 1) with those that bound both Hsp70 and Hsp90 chaperones (Supplemental Fig. 2). In this limited data set, we did not find any distinguishable characteristics that were common or unique to one group to streamline our assay. The chemical structures of some compounds suggest that they likely fluoresce and interfere with the thermofluor assay. Fluorescent and aggregation artifacts would also be encountered in the Hsp90 counter screen and likely serve to select out compounds with these properties. However, a nonprotein control in future studies would more definitively rule out fluorescent compounds. In addition, for some compounds, we observed odd Hill slope equivalents (Fig. 4, C, D, and G), which might suggest that the compound interacts with the dye or that the compound binds to Hsp70 on multiple sites. Further analysis of these observations in our search for more compounds may help to delineate better ways to carry out the thermofluor assays. It is noteworthy that a protocol for optimizing data collection for thermofluor experiments has been described (Wu et al, 2023, 2024).

3.3. Hsp70-dependent ubiquitination of apo-nNOS to assess hit compounds

To assess the functional effects of the Hsp70 thermostabilizers, we used an in vitro system containing purified Hsp70 and CHIP, a C-terminus of the Hsc70-interacting protein that is a chaperone-dependent E3 ubiquitin ligase, along with all the other components necessary for ubiquitination, including E1 ubiquitin–conjugating enzyme, E2 ubiquitin ligase, and ubiquitin. Interestingly, this system preferentially ubiquitinates the misfolded heme-deficient nNOS (apo-nNOS) over that of the native heme-sufficient, holo-nNOS (Davis et al, 2020a). Moreover, not only is the ubiquitination fully dependent on CHIP, but as described below, it is also dependent on the nucleotide state of Hsp70. We used a FLAG-tagged apo-nNOS that greatly facilitates the quantification of apo-nNOS ubiquitination by the use of an anti-FLAG–based sandwich ELISA method and anti–ubiquitin-HRP enzyme (Davis et al, 2020a). As shown in Fig. 5A, apo-nNOS ubiquitination by this system is enhanced by Hsp40, an Hsp70 cochaperone, in a concentration-dependent manner. This is

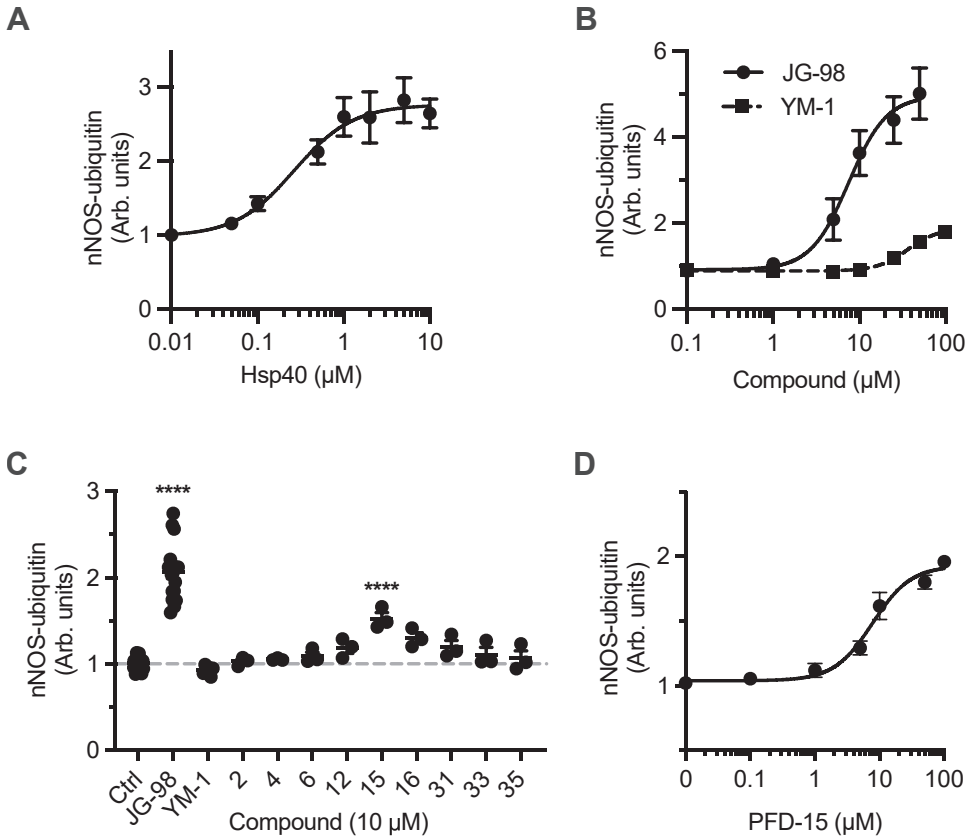

Fig. 5. Purified protein ubiquitination reaction coupled with an ELISA was used to characterize the effect of Hsp70 modulators on Hsp70:CHIP-dependent ubiquitination of nNOS in vitro. As described in the *Materials and methods*, FLAG–apo-nNOS was incubated with the purified protein ubiquitination reaction mixture and immobilized on an anti-FLAG 96-well plate. The plate was then probed with an antiubiquitin antibody conjugated to HRP, and HRP activity was quantified. (A) The Hsp70 cochaperone Hsp40, known to promote hydrolysis of ATP to ADP by Hsp70, increases nNOS ubiquitination. (B) The small molecules YM-01 (dashed line) and JG-98 (solid line), known modulators of Hsp70, also increase the ubiquitination of apo-nNOS in vitro. Values are reported as the average signal relative to untreated apo-nNOS ± SD ($n = 3–6$). (C) The ubiquitination reaction mixture was treated with 10 μM of each Hsp70 selective thermostabilizer or either JG-98 or YM-01 as controls (Ctrl). One small molecule, PFD-15, caused a statistically significant increase in nNOS ubiquitination. Ordinary one-way ANOVA followed by Dunnett's multiple comparisons test was used to compare vehicle Ctrl treatment with all other treatment conditions ($n = 3–17$). ****$P < .0001$. (D) PFD-15 caused concentration-dependent increases in nNOS ubiquitination. Values are reported as relative to untreated apo-nNOS and represent means ± SD ($n = 3$). Arb. units, arbitrary units.

consistent with the interpretation that Hsp40 enhances the hydrolysis of Hsp70-bound ATP to ADP, favoring the ADP state of Hsp70 and CHIP binding. The binding of CHIP to Hsp70 then facilitates the ubiquitination of Hsp70-bound client proteins. In contrast, the ubiquitination of apo-nNOS has been shown to be inhibited by BAG-1M, a nucleotide exchange factor that promotes the release of ADP from Hsp70, thus limiting the stability of the ADP state (Davis et al, 2020a). Thus, this in vitro system is sensitive to factors that affect the formation or stability of the ADP state of Hsp70 and is a facile quantitative method to determine if the hit compounds identified in the thermal shift assay elicit functional effects on misfolded client ubiquitination. As proof of this, we selected 2 small-molecule rhodacyanine dye derivatives, JG-98 and YM-01, that have been shown to bind Hsp70, stabilize the ADP conformation of Hsp70, and enhance CHIP-dependent ubiquitination as positive controls (Rousaki et al, 2011; Wang et al, 2013). As shown in Fig. 5B, JG-98 (circles) increased ubiquitination of apo-nNOS in a concentration-dependent manner with an EC_{50} value of approximately 8 μM, consistent with earlier observations (Davis et al, 2020a). Also consistent with previous reports, YM-01 was less potent and efficacious than JG-98, with an EC_{50} value of approximately 36 μM (Li et al, 2015). Thus, these findings provide the basis for using this in vitro ubiquitination assay to select compounds of interest.

In Fig. 5C, we assessed the ability of the 9 hit compounds identified above to thermostabilized Hsp70 in the in vitro ubiquitination assay. At a concentration of 10 μM, only the positive control, JG-98, and 1 of the 9 compounds, PFD-15, caused an increase in apo-nNOS ubiquitination. It is noteworthy that YM-01 at this concentration had little effect. As shown in Fig. 5D, PFD-15 caused a concentration-dependent increase in nNOS ubiquitination with an EC_{50} of approximately 8 μM. Thus, of the 9 compounds that selectively thermostabilized Hsp70, one compound (PFD-15) was found to enhance the Hsp70-dependent ubiquitination of a client protein in vitro.

3.4. Effect of PFD-15 on misfolded nNOS in HEK293 cells

The in vitro system used apo-nNOS as the misfolded client protein, but to make the heme-deficient apo-nNOS in cells required inhibition of heme synthesis for an extended period. Thus, we initially chose to use a C331A mutant of nNOS that is catalytically competent but has a slightly perturbed substrate binding site with decreased affinity for tetrahydrobiopterin (Martásek et al, 1998). Our laboratory has shown that C331A nNOS expressed in cells is more susceptible to ubiquitination than the wild-type enzyme (Clapp et al, 2010). Interestingly, the C331A nNOS is stabilized from ubiquitination to that near the wild-type enzyme by treatment of cells with compounds that bind the heme active site of nNOS (Clapp et al, 2010). These findings have led to the notion that C331A nNOS has a misfolded active site cleft that can be rescued by binding a

heme ligand. Although it is likely that the apo-nNOS form is more misfolded than the C331A nNOS, this mutant nonetheless serves as a useful model for testing Hsp70 modulators on degradation of misfolded client proteins.

As shown in Fig. 6A, treatment of HEK293 cells stably expressing C331A nNOS with 40 μM PFD-15 caused a time-dependent loss in the steady-state level of C331A nNOS protein over 48 hours (open squares). There was no effect over that duration in untreated cells (closed square). The loss of C331A nNOS at 24 hours was examined further and found to be dependent on the concentration of PFD-15 (open squares) over a range of 1–40 μM (Fig. 6B). Wild-type nNOS was not affected by PFD-15 over the same concentration range (closed squares). Taken together, this suggests a selective effect on the misfolded nNOS by PFD-15. Viability decreased slightly from 96% to 85% when C331A-nNOS– or wild-type nNOS–expressing cells were treated with 40 μM PFD-15 for 24 hours (Supplemental Fig. 3). However, there was no statically significant difference in cell viability between wild-type nNOS or C331A-nNOS treated with 40 μM PFD-15. Thus, we conclude that cell death is not the cause of the decrease in C331A-nNOS. As shown in Fig. 6C, pretreatment of cells for 2 hours with the proteasome inhibitor lactacystin (10 μM) protected from the loss of C331A nNOS due to 40 μM of PFD-15 (lane 3 vs lane 4), indicating that the loss of protein is due to proteasomal degradation. This is consistent with the reports that C331A nNOS is degraded by the proteasome in cells (Clapp et al, 2010). Client proteins may also undergo autophagic turnover, but studies with bafilomycin (100 nM) indicate that this is not a predominant pathway (Supplemental Fig. 4). As shown in Fig. 6D, pretreatment of cells for 2 hours with 200 μM N^G-nitro-L-arginine (L-NNA), a slowly reversible nNOS inhibitor, also protected against

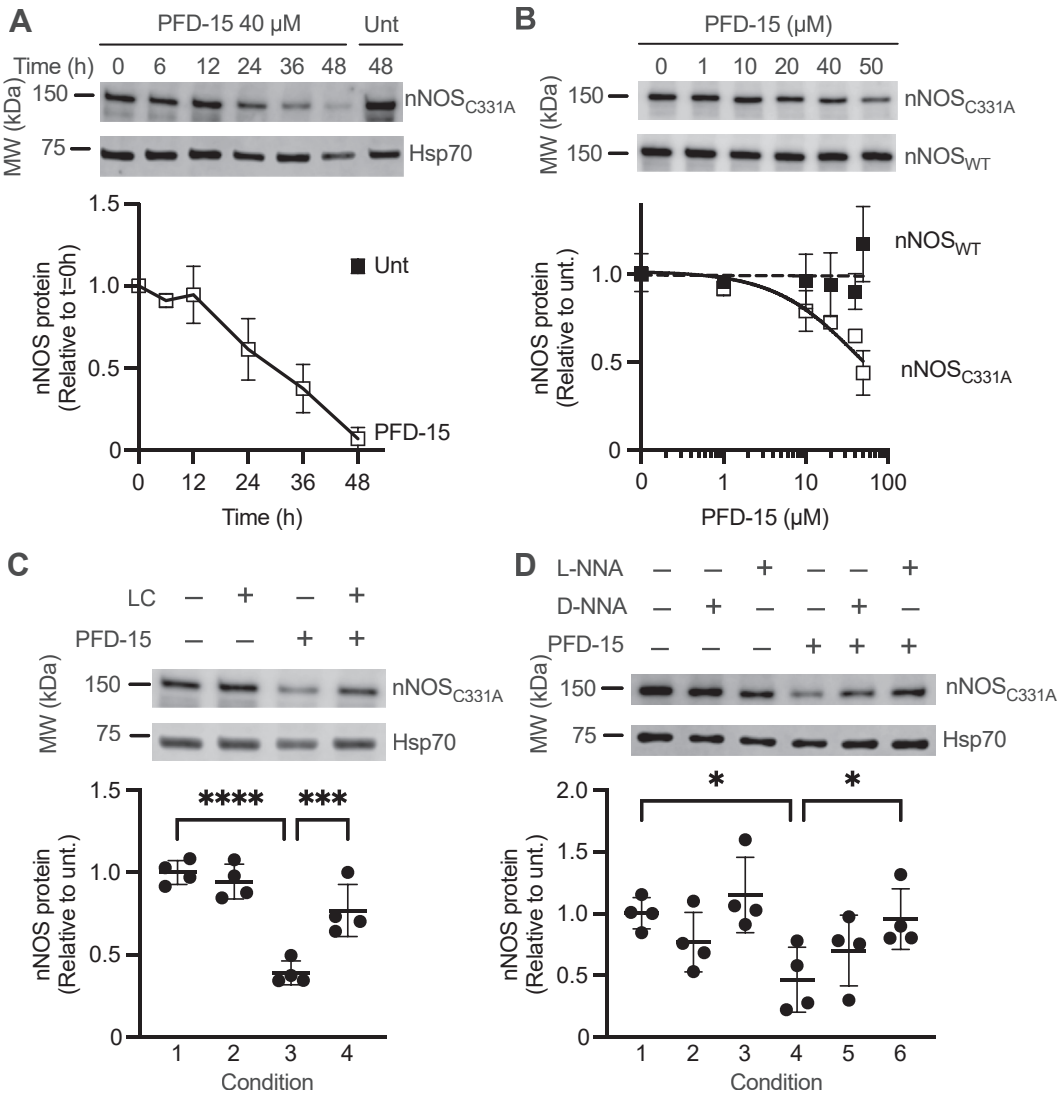

Fig. 6. A small-molecule Hsp70 thermostabilizer promotes degradation of misfolded nNOS in intact cells. (A) Cells stably expressing C331A-nNOS were treated with 40 μM PFD-15 (open squares) or vehicle (closed square) for the indicated times. A time-dependent loss of C331A-nNOS protein levels was observed. Values are reported as average nNOS protein relative to t = 0 ± SD ($n = 3$) from 3 individual experiments. (B) Wild-type (WT, closed squares) or C331A-nNOS (open squares) -expressing cell lines were treated with increasing concentrations of PFD-15 for 24 hours. A concentration-dependent decrease of nNOS protein levels was observed in C331A-nNOS–expressing cells (open squares) but not in WT-nNOS cells (closed squares). Values are reported as average nNOS protein relative to untreated (Unt) ± SD ($n = 4$) from 4 individual experiments. (C) C331A-nNOS cells were pretreated with lactacystin (LC, 10 μM) for 2 hours before being treated with 40 μM PFD-15 for a total of 24 hours. (D) Cells expressing C331A-nNOS were grown in reduced L-arginine (200 μM) media for 48 hours. They were then pretreated for 2 hours with vehicle, N^G-nitro-D-arginine (D-NNA) (200 μM), or L-NNA (200 μM) before being treated with PFD-15 (40 μM) for a total of 24 hours. Values are reported as average nNOS protein relative to Unt ± SD ($n = 4$) from 4 individual experiments. Ordinary one-way ANOVA followed by Dunnett's multiple comparisons test was used to compare PFD-15 treatment with all other conditions. ****$P \leq .0001$; ***$P = .0009$; *$P < .05$. MW, molecular weight.

the loss of C331A nNOS caused by PFD-15 (lane 4 vs lane 6), while pretreatment with the inactive isomer, N^G-nitro-D-arginine, did not (lane 4 vs lane 5). L-NNA binding stabilizes the heme binding pocket (Martásek et al, 1998) and protects against Hsp70:CHIP-mediated ubiquitination and proteasomal degradation (Clapp et al, 2010). This stereospecific rescue by L-NNA is entirely consistent with the notion that PFD-15 selectively targets the misfolded nNOS over that of the native nNOS.

3.5. PFD-15 enhances the association of CHIP to heme-deficient apo-nNOS

Apo-nNOS is a better-misfolded client to examine stable binding of chaperones to nNOS (Morishima et al, 2023). In the course of our studies, we developed a tetracycline-inducible nNOS HEK293 cell system where we could induce expression of nNOS in the presence of an inhibitor to heme synthesis to efficiently make apo-nNOS. As shown in Fig. 7A, immunoisolation of apo-nNOS from tetracycline-treated cells showed nNOS associated with Hsp70 and CHIP (lane 2 vs lane 1). Furthermore, treatment of the cells with 40 μM PFD-15 for 2 hours increased both Hsp70 and CHIP bound to nNOS (lane 3 and quantitation in Fig. 7B). We have verified that 40 μM PFD-15 causes a loss of about half of the apo-nNOS at 24 hours (Supplemental Fig. 5), consistent with that found for C331A nNOS, indicating that apo-nNOS acts similarly to C331A nNOS.

Studies in the purified protein system, similar to that used to study the ubiquitination of apo-nNOS above, showed an increased association of CHIP to apo-nNOS due to treatment with PFD-15 (Fig. 7C, lanes 1–3). As shown in Fig. 7D, the densities were quantified, and there was a clear increase in CHIP but not Hsp70. We do not know the reason for this difference between the in vitro and cellular systems in Hsp70 binding. However, the increased binding of CHIP to nNOS caused by PFD-15 is abolished by Bag-1M, strongly suggesting that Hsp70 is involved (Fig. 7C lane 4 and D). These findings are consistent with a previous study showing that BAG-1M inhibits Hsp70:CHIP-dependent ubiquitination of apo-nNOS (Davis et al, 2020a). To further investigate if Hsp70 is affected by PFD-15, we showed by cellular thermal shift assay (Supplemental Methods) that a slight stabilization of Hsp70 could be observed when cells were treated with PFD-15 at 40 μM (Supplemental Fig. 6). The stabilization was moderate, and we conclude that more potent structural analogs are needed for measurements of direct binding to Hsp70. However, taken together, the results strongly indicate that PFD-15 enhances association of CHIP to misfolded nNOS through actions on Hsp70.

3.6. PFD-15 enhances ubiquitination of other misfolded proteins

We treated HEK293 cells not expressing nNOS with PFD-15 (40 μM) and examined the amount of ubiquitin adducts by

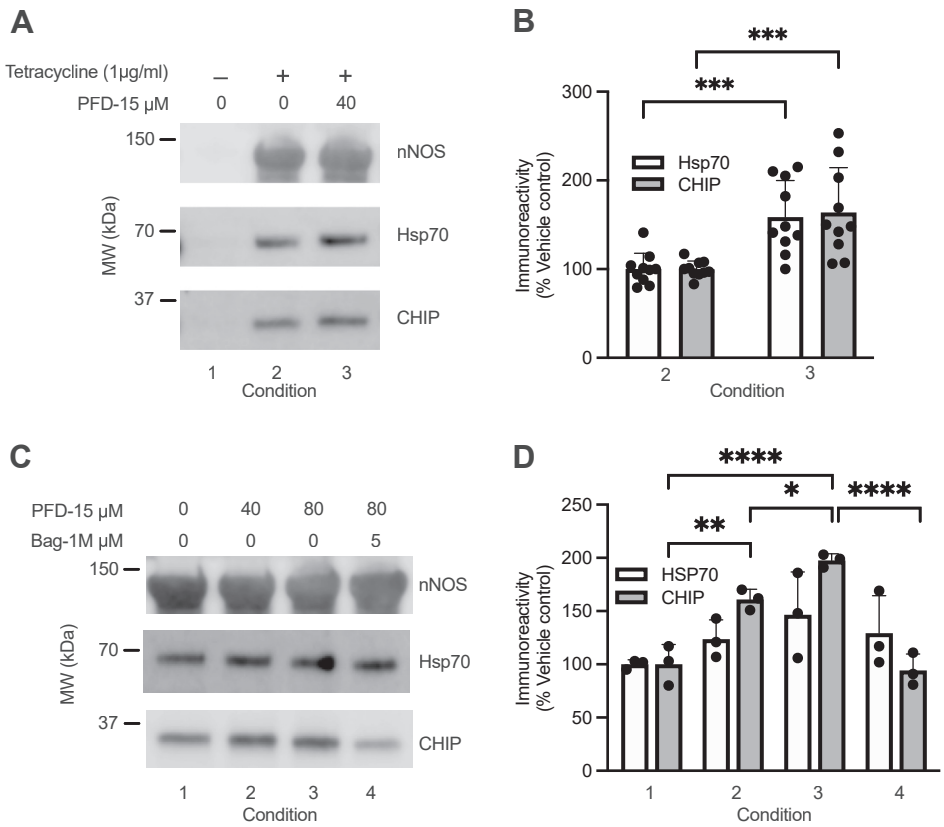

Fig. 7. PFD-15 promotes the association of CHIP with misfolded nNOS. (A) PFD-15 treatment of HEK293 cells expressing apo-nNOS increases the association of Hsp70 and CHIP. HEK293 tetracycline-inducible nNOS cells were treated with succinylacetone to form heme-deficient apo-nNOS and then treated with PFD-15 (40 μM) for 2 hours. The cells were harvested and lysed, and the apo-nNOS immunoprecipitated and the associated Hsp70 and CHIP were blotted as described in the *Materials and methods*. The blots were quantified in (B). Open bars, Hsp70; closed bars, CHIP. Values are reported as the average of the target protein relative to vehicle control ± SD ($n = 10$) from 4 individual experiments. A two-tailed unpaired t test was used. ***$P < .001$. (C) PFD-15 enhances CHIP binding to apo-nNOS in a purified system containing Hsp70 and CHIP. A purified reaction mixture containing apo-nNOS, Hsp70, and CHIP was incubated with PFD-15 at the indicated concentrations, and the associated Hsp70 and CHIP were western blotted as described in the *Materials and methods*. Bag-1M was added to show specificity for Hsp70. The blots were quantified in (D). Open bars, Hsp70; closed bars, CHIP. Values are reported as target protein relative to vehicle control ± SD ($n = 3$) from 3 individual experiments. Ordinary one-way ANOVA followed by Tukey's multiple comparisons test was used to compare target protein expression in all conditions. *$P < .05$; **$P < .01$; ****$P < .0001$. MW, molecular weight.

western blotting with an antiubiquitin antibody. As shown in Fig. 8A, PFD-15 treatment alone did not cause a large change in the immunodetectable ubiquitin adducts (lane 2 vs lane 1). However, when the cells were warmed to 42 °C for 30 minutes to provide a short heat shock in the hopes of misfolding some native proteins, PFD-15 caused a large increase in immunodetectable ubiquitin adducts (lane 4 vs lane 3). Taken together, the results are consistent with the notion that PFD-15 selectively enhances the ubiquitination of misfolded proteins.

4. Discussion

We have developed a series of assays to identify compounds that target Hsp70 and enhance the degradation of client proteins. In the course of studies on Hsp70, we found that ADP caused a remarkably large increase in the Tm of Hsp70 in a thermal shift-based assay with SYPRO Orange. Since compounds that stabilize the ADP conformation of Hsp70 were found to enhance ubiquitination of client proteins (Wang et al, 2013), we wondered if this assay might be used to identify similar Hsp70 modulators. At the very least, we reasoned that this facile assay could be used to identify compounds that bind and cause a conformational change in Hsp70. We screened 44,447 small molecules from the Maybridge and ChemDiv libraries using this Hsp70 thermostability assay as our primary screen, and we identified 2126 hits (Fig. 1). Of these compounds, about a third were tested for concentration-dependent responses, and we obtained 129 hits. Of these compounds, only 35 compounds were repurchased in fresh powder form, and concentration-response studies validated only about half of these compounds. The Hsp90 counter screen gave 9 compounds selective for Hsp70 for further biochemical testing. Thus, because we did not fully test the entire set of hits at each step, it is likely that many more compounds in the library have the ability to bind to Hsp70.

To our knowledge, this is the first time a thermal shift screen was used to find compounds that bind to Hsp70. Some previous high-throughput screens directed against Hsp70 have targeted nucleotide-binding sites using fluorescein-labeled ATP in a fluorescence polarization assay to identify adenosine-derived inhibitors (Williamson et al, 2009) or targeting protein-protein interactions with cochaperones using ATPase activity as a marker (Fewell et al, 2004; Chang et al, 2008; Miyata et al, 2010; Chang et al, 2011; Taylor et al, 2018) or employed a fluorescent-linked enzyme chemoproteomic strategy for compounds that interact at the nucleotide-binding site (Howe et al, 2014). Virtual screening methods have also been used to synthesize small molecules that bind the nucleotide-binding domain of Hsp70 (Rodina et al, 2013; Zeng et al, 2015) or the peptide binding site on the substrate binding domain (Haney et al, 2009). These screens were directed, for the most part, at finding anticancer agents.

Unlike these other high-throughput screening efforts, we designed secondary assays to directly probe the protein quality control function of Hsp70 against misfolded client proteins. We used a quantitative ELISA assay that directly measures the Hsp70:CHIP-dependent ubiquitination and is sensitive to the misfolded state of the client protein (Davis et al, 2020a). We have previously shown that a heme-deficient or apo-form of nNOS (apo-nNOS) is a preferred substrate for Hsp70 recognition and CHIP-dependent ubiquitination (Davis et al, 2020a). Of the 9 compounds tested in this in vitro assay, one compound (PFD-15) was found to enhance ubiquitination of apo-nNOS. It is noteworthy that these assays contained 1 mM ATP and were likely selected against compounds that interact at the nucleotide-binding site.

To test the effects of Hsp70 modulators in cells, we chose an established cellular model to address the selectivity for the misfolded state by using a C331A point mutant of nNOS (C331A nNOS) that is susceptible to Hsp70:CHIP-dependent ubiquitination (Clapp et al, 2010). Although we could have generated apo-nNOS in cells for these studies, it would require extensive treatment with an inhibitor to heme synthesis. Moreover, by using the mutant nNOS, we could take advantage of the ability of tight-binding substrate analogs or ligands to the heme group of C331A nNOS to stabilize the protein to a conformation more like the native enzyme and determine the effects of Hsp70 modulators on protein quality control. That is, we can ask if modulation of Hsp70 enhances only misfolded client protein degradation or also enhances native protein degradation. Thus, through the series of assays, we could clearly show that PFD-15 predominantly affected the misfolded mutant form of nNOS, sparing the native protein in cells. We believe that this series

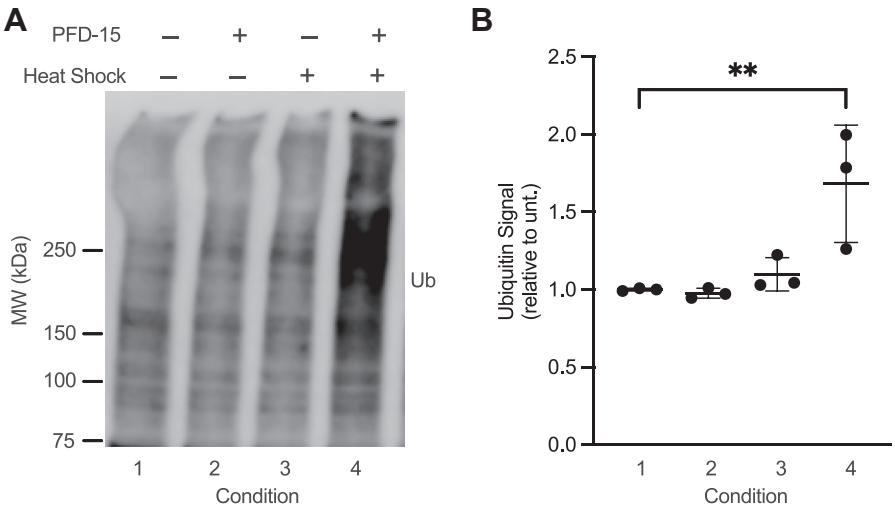

Fig. 8. PFD-15 promotes the ubiquitination of misfolded proteins in HEK293 cells. (A) PFD-15 increases ubiquitin conjugates in PFD-15–treated cells only after a short heat shock treatment. HEK293T cells not transfected with nNOS were pretreated with PFD-15 for 30 minutes and then subjected to heat shock of 42 °C for 30 minutes as indicated. Cells were treated and lysed, and samples were western blotted for ubiquitin as described in the *Materials and methods*. The western blot for proteins below 75 kDa, which contributed to less than 20% of the total signal in all lanes and did not change in all conditions, is not shown. The total density of all ubiquitin bands above 75kDa was quantified in (B). Values are reported as average ubiquitin protein relative to control ± SD ($n = 3$). Ordinary one-way ANOVA followed by Dunnett's multiple comparisons test was used to compare condition 1 with all other conditions. $^{**}P < .01$. MW, molecular weight; unt, untreated.

of assays effectively selects for Hsp70 modulators that enhance misfolded client protein degradation but also addresses whether the protein quality control function of the Hsp90:Hsp70 chaperone machinery is maintained.

To delineate the potential mechanism of the action of PFD-15, we investigated the role of CHIP, an E3-ubiquitin ligase that is known to ubiquitinate nNOS in cells (Peng et al, 2004). We found that treatment of HEK293 cells with PFD-15 enhances binding of Hsp70 and CHIP to apo-nNOS, which forms more stable complexes with chaperones. PFD-15 also enhanced CHIP binding to apo-nNOS in an in vitro system containing only purified Hsp70 and CHIP. Moreover, the increased binding of CHIP to apo-nNOS caused by PFD-15 was abrogated by the treatment with Bag-1M, which binds to Hsp70 to accelerate ADP release. Since CHIP binds to the ADP-bound state of Hsp70, this strongly implicates Hsp70 in the enhanced CHIP binding to apo-nNOS. In addition, cellular thermal shift assay studies further supported the in vitro thermofluor assays to indicate that PFD-15 acts through Hsp70. Thus, taken together, these studies strongly suggest that PFD-15 binds to Hsp70 to facilitate CHIP binding and enhance ubiquitination of the client protein, which, in our case, is misfolded nNOS. This mechanism was further corroborated by the observation that PFD-15 enhanced overall ubiquitination when cells were heat-shocked for a short period to form misfolded proteins. Most importantly, no increase in ubiquitination was found in non−heat-shocked cells after treatment with PFD-15. Moreover, only misfolded forms of nNOS, namely the C331A nNOS or apo-nNOS, were affected by PFD-15, leaving wild-type nNOS unaffected. Thus, PFD-15 does not cause the massive degradation of cellular proteins but rather enhances the protein triage mechanism by selective degradation of misfolded forms of client proteins through actions on Hsp70 and CHIP. Further work is needed to enhance the potency of the compound for animal studies, but the current studies indicate the potential for discovering novel molecules directed at Hsp70 and control of protein quality through the methods described here.

Abbreviations

CHIP, C-terminus of Hsc70 interacting protein; DMEM, Dulbecco's modified Eagle's medium; HEK293, human embryonic kidney 293; HRP, horseradish peroxidase; HIP, Hsp70 interacting protein; Hsp70, heat shock protein 70; Hsp90, heat shock protein 90; L-NNA, N^G-nitro-L-arginine; nNOS, neuronal NO synthase; PFD-15, protein folding disease compound 15; polyQ-AR, polyglutamine tract containing androgen receptor; RIPA, radioimmunoprecipitation assay; Tm, melting temperature.

Acknowledgments

We thank Aaron Robida and the University of Michigan's Life Sciences Institute Center for Chemical Genomics for help running the high-throughput screen and with the interpretation of the screening data.

Financial support

This work was supported by National Institutes of Health [Grants GM077430 and GM153714] (to Y.O.) and [Grant NS119873] (to A.P.L.). This project is a component of the University of Michigan Medical School's Protein Folding Disease Research Initiative. A.M.G. is a trainee of the University of Michigan Training Program in Translational Science (National Institutes of Health T32-GM141840) and a Department of Pharmacology Lucchesi Fellow.

Conflict of interest

The authors declare no conflicts of interest.

Data availability

All other data supporting the findings of this study are available within the article and/or its Supplemental Material.

Authorship contributions

Participated in research design: Garcia, Davis, Zhang, Alt, Lieberman, Osawa.

Conducted experiments: Garcia, Davis, Martinez-Ramos, Morishima, Lau, Xu, Sunil.

Contributed new reagents or analytic tools: Morishima, Lau, Alt.

Performed data analysis: Garcia, Davis, Morishima.

Wrote or contributed to the writing of the manuscript: Garcia, Davis, Morishima, Lau, Zhang, Alt, Lieberman, Osawa.

Supplemental material

This article has supplemental material available at molpharm.aspetjournals.org.

References

Ambrose AJ and Chapman E (2021) Function, therapeutic potential, and inhibition of Hsp70 chaperones. *J Med Chem* **64**:7060−7082.

Ballinger CA, Connell P, Wu Y, Hu Z, Thompson LJ, Yin LY, and Patterson C (1999) Identification of CHIP, a novel tetratricopeptide repeat-containing protein that interacts with heat shock proteins and negatively regulates chaperone functions. *Mol Cell Biol* **19**:4535−4545.

Bender AT, Silverstein AM, Demady DR, Kanelakis KC, Noguchi S, Pratt WB, and Osawa Y (1999) Neuronal nitric-oxide synthase is regulated by the hsp90-based chaperone system in vivo. *J Biol Chem* **274**:1472−1478.

Bredt DS, Hwang PM, Glatt CE, Lowenstein C, Reed RR, and Snyder SH (1991) Cloned and expressed nitric oxide synthase structurally resembles cytochrome P-450 reductase. *Nature* **351**:714−718.

Chang L, Bertelsen EB, Wisén S, Larsen EM, Zuiderweg ERP, and Gestwicki JE (2008) High-throughput screen for small molecules that modulate the ATPase activity of the molecular chaperone DnaK. *Anal Biochem* **372**:167−176.

Chang L, Miyata Y, Ung PMU, Bertelsen EB, McQuade TJ, Carlson HA, Zuiderweg ERP, and Gestwicki JE (2011) Chemical screens against a reconstituted multiprotein complex: myricetin blocks DnaJ regulation of DnaK through an allosteric mechanism. *Chem Biol* **18**:210−221.

Clapp KM, Peng HM, Morishima Y, Lau M, Walker VJ, Pratt WB, and Osawa Y (2010) C331A mutant of neuronal nitric-oxide synthase is labilized for Hsp70/CHIP (C terminus of HSC70-interacting protein)-dependent ubiquitination. *J Biol Chem* **285**:33642−33651.

Congdon EE, Wu JW, Myeku N, Figueroa YH, Herman M, Marinec PS, Gestwicki JE, Dickey CA, Yu WH, and Duff KE (2012) Methylthioninium chloride (methylene blue) induces autophagy and attenuates tauopathy in vitro and in vivo. *Autophagy* **8**:609−622.

Davis AK, McMyn NF, Lau M, Morishima Y, and Osawa Y (2020a) Hsp70:CHIP ubiquitinates dysfunctional but not native neuronal NO synthase. *Mol Pharmacol* **98**:243−249.

Davis AK, Pratt WB, Lieberman AP, and Osawa Y (2020b) Targeting Hsp70 facilitated protein quality control for treatment of polyglutamine diseases. *Cell Mol Life Sci* **77**:977−996.

Dittmar KD, Hutchison KA, Owens-Grillo JK, and Pratt WB (1996) Reconstitution of the steroid receptor.hsp90 heterocomplex assembly system of rabbit reticulocyte lysate. *J Biol Chem* **271**:12833−12839.

Echtenkamp FJ, Ishida R, Rivera-Marquez GM, Maisiak M, Johnson OT, Shrimp JH, Sinha A, Ralph SJ, Nisbet I, and Cherukuri MK, et al. (2023) Mitoribosome sensitivity to HSP70 inhibition uncovers metabolic liabilities of castration-resistant prostate cancer. *PNAS Nexus* **2**:pgad115.

Fewell SW, Smith CM, Lyon MA, Dumitrescu TP, Wipf P, Day BW, and Brodsky JL (2004) Small molecule modulators of endogenous and co-chaperone-stimulated Hsp70 ATPase activity. *J Biol Chem* **279**:51131−51140.

Gestwicki JE and Shao H (2019) Inhibitors and chemical probes for molecular chaperone networks. *J Biol Chem* **294**:2151−2161.

Gong B, Radulovic M, Figueiredo-Pereira ME, and Cardozo C (2016) The ubiquitin-proteasome system: potential therapeutic targets for Alzheimer's disease and spinal cord injury. *Front Mol Neurosci* **9**:4.

Gupta A, Bansal A, and Hashimoto-Torii K (2020) HSP70 and HSP90 in neurodegenerative diseases. *Neurosci Lett* **716**:134678.
Haney CM, Schneider C, Beck B, Brodsky JL, and Dömling A (2009) Identification of Hsp70 modulators through modeling of the substrate binding domain. *Bioorg Med Chem Lett* **19**:3828–3831.
Howe MK, Bodoor K, Carlson DA, Hughes PF, Alwarawrah Y, Loiselle DR, Jaeger AM, Darr DB, Jordan JL, and Hunter LM, et al. (2014) Identification of an allosteric small-molecule inhibitor selective for the inducible form of heat shock protein 70. *Chem Biol* **21**:1648–1659.
Lazarev VF, Sverchinsky DV, Mikhaylova ER, Semenyuk PI, Komarova EY, Niskanen SA, Nikotina AD, Burakov AV, Kartsev VG, and Guzhova IV, et al. (2018) Sensitizing tumor cells to conventional drugs: HSP70 chaperone inhibitors, their selection and application in cancer models. *Cell Death Dis* **9**:41.
Li X, Colvin T, Rauch JN, Acosta-Alvear D, Kampmann M, Dunyak B, Hann B, Aftab BT, Murnane M, and Cho M, et al. (2015) Validation of the Hsp70–Bag3 protein–protein interaction as a potential therapeutic target in cancer. *Mol Cancer Ther* **14**:642–648.
Li ZN and Luo Y (2023) HSP90 inhibitors and cancer: prospects for use in targeted therapies (review). *Oncol Rep* **49**:6.
Martásek P, Miller RT, Liu Q, Roman LJ, Salerno JC, Migita CT, Raman CS, Gross SS, Ikeda-Saito M, and Masters BS (1998) The C331A mutant of neuronal nitric-oxide synthase is defective in arginine binding. *J Biol Chem* **273**:34799–34805.
Mehta RK, Pal S, Kondapi K, Sitto M, Dewar C, Devasia T, Schipper MJ, Thomas DG, Basrur V, and Pai MP, et al. (2020) Low-dose Hsp90 inhibitor selectively radiosensitizes HNSCC and pancreatic xenografts. *Clin Cancer Res* **26**:5246–5257.
Miyata Y, Chang L, Bainor A, Mcquade TJ, Walczak CP, Zhang Y, Larsen MJ, Kirchhoff P, and Gestwicki JE (2010) High-throughput screen for *Escherichia coli* heat shock protein 70 (Hsp70/DnaK): ATPase assay in low volume by exploiting energy transfer. *J Biomol Screen* **15**:1211–1219.
Morishima Y, Lau M, Pratt WB, and Osawa Y (2023) Dynamic cycling with a unique Hsp90/Hsp70-dependent chaperone machinery and GAPDH is needed for heme insertion and activation of neuronal NO synthase. *J Biol Chem* **299**:102856.
Morishima Y, Zhang H, Lau M, and Osawa Y (2016) Improved method for assembly of hemeprotein neuronal NO-synthase heterodimers. *Anal Biochem* **511**:24–26.
Palleros DR, Shi L, Reid KL, and Fink AL (1994) hsp70-protein complexes. Complex stability and conformation of bound substrate protein. *J Biol Chem* **269**:13107–13114.
Peng HM, Morishima Y, Jenkins GJ, Dunbar AY, Lau M, Patterson C, Pratt WB, and Osawa Y (2004) Ubiquitylation of neuronal nitric-oxide synthase by CHIP, a chaperone-dependent E3 ligase. *J Biol Chem* **279**:52970–52977.
Pratt WB, Gestwicki JE, Osawa Y, and Lieberman AP (2015) Targeting Hsp90/Hsp70-based protein quality control for treatment of adult onset neurodegenerative diseases. *Annu Rev Pharmacol Toxicol* **55**:353–371.
Rodina A, Patel PD, Kang Y, Patel Y, Baaklini I, Wong MJH, Taldone T, Yan P, Yang C, and Maharaj R, et al. (2013) Identification of an allosteric pocket on human Hsp70 reveals a mode of inhibition of this therapeutically important protein. *Chem Biol* **20**:1469–1480.
Rousaki A, Miyata Y, Jinwal UK, Dickey CA, Gestwicki JE, and Zuiderweg ERP (2011) Allosteric drugs: the interaction of antitumor compound MKT-077 with human Hsp70 chaperones. *J Mol Biol* **411**:614–632.
Shao H, Li X, Hayashi S, Bertron JL, Schwarz DMC, Tang BC, and Gestwicki JE (2021) Inhibitors of heat shock protein 70 (Hsp70) with enhanced metabolic stability reduce Tau levels. *Bioorg Med Chem Lett* **41**:128025.
Shao H, Li X, Moses MA, Gilbert LA, Kalyanaraman C, Young ZT, Chernova M, Journey SN, Weissman JS, and Hann B, et al. (2018) Exploration of benzothiazole rhodacyanines as allosteric inhibitors of protein–protein interactions with heat shock protein 70 (Hsp70). *J Med Chem* **61**:6163–6177.
Talaei S, Mellatyar H, Asadi A, Akbarzadeh A, Sheervalilou R, and Zarghami N (2019) Spotlight on 17-AAG as an Hsp90 inhibitor for molecular targeted cancer treatment. *Chem Biol Drug Des* **93**:760–786.
Taylor IR, Dunyak BM, Komiyama T, Shao H, Ran X, Assimon VA, Kalyanaraman C, Rauch JN, Jacobson MP, and Zuiderweg ERP, et al. (2018) High-throughput screen for inhibitors of protein–protein interactions in a reconstituted heat shock protein 70 (Hsp70) complex. *J Biol Chem* **293**:4014–4025.
Venediktov AA, Bushueva OY, Kudryavtseva VA, Kuzmin EA, Moiseeva AV, Baldycheva A, Meglinski I, and Piavchenko GA (2023) Closest horizons of Hsp70 engagement to manage neurodegeneration. *Front Mol Neurosci* **16**:1230436.
Wang AM, Miyata Y, Klinedinst S, Peng HM, Chua JP, Komiyama T, Li X, Morishima Y, Merry DE, and Pratt WB, et al. (2013) Activation of Hsp70 reduces neurotoxicity by promoting polyglutamine protein degradation. *Nat Chem Biol* **9**:112–118.
Wang AM, Morishima Y, Clapp KM, Peng HM, Pratt WB, Gestwicki JE, Osawa Y, and Lieberman AP (2010) Inhibition of Hsp70 by methylene blue affects signaling protein function and ubiquitination and modulates polyglutamine protein degradation. *J Biol Chem* **285**:15714–15723.
Williamson DS, Borgognoni J, Clay A, Daniels Z, Dokurno P, Drysdale MJ, Foloppe N, Francis GL, Graham CJ, and Howes R, et al. (2009) Novel adenosine-derived inhibitors of 70 kDa heat shock protein, discovered through structure-based design. *J Med Chem* **52**:1510–1513.
Wu T, Gale-Day ZJ, and Gestwicki JE (2024) DSFworld: a flexible and precise tool to analyze differential scanning fluorimetry data. *Protein Sci* **33**:e5022.
Wu T, Hornsby M, Zhu L, Yu JC, Shokat KM, and Gestwicki JE (2023) Protocol for performing and optimizing differential scanning fluorimetry experiments. *STAR Protoc* **4**:102688.
You J and Pickart CM (2001) A HECT domain E3 enzyme assembles novel polyubiquitin chains. *J Biol Chem* **276**:19871–19878.
Young ZT, Rauch JN, Assimon VA, Jinwal UK, Ahn M, Li X, Dunyak BM, Ahmad A, Carlson GA, and Srinivasan SR, et al. (2016) Stabilizing the Hsp70-Tau complex promotes turnover in models of tauopathy. *Cell Chem Biol* **23**:992–1001.
Zeng Y, Cao R, Zhang T, Li S, and Zhong W (2015) Design and synthesis of piperidine derivatives as novel human heat shock protein 70 inhibitors for the treatment of drug-resistant tumors. *Eur J Med Chem* **97**:19–31.
Zhang JH, Chung TD, and Oldenburg KR (1999) A simple statistical parameter for use in evaluation and validation of high throughput screening assays. *J Biomol Screen* **4**:67–73.
Zhu Y, Hon T, Ye W, and Zhang L (2002) Heme deficiency interferes with the Ras-mitogen-activated protein kinase signaling pathway and expression of a subset of neuronal genes1. *Cell Growth Differ* **13**:431–439.